ELSEVIER

Biophysical Chemistry 123 (2006) 29–39

Biophysical Chemistry

http://www.elsevier.com/locate/biophyschem

Interaction of local anesthetics with a peptide encompassing the IV/S4–S5 linker of the Na^+ channel

Leonardo F. Fraceto [a,b,1], Sérgio Oyama Jr. [a], Clóvis R. Nakaie [c], Alberto Spisni [a,d], Eneida de Paula [b,*], Thelma A. Pertinhez [a,d,*]

[a] *Center of Molecular and Structural Biology, LNLS, Campinas, Brazil*
[b] *Department of Biochemistry, Institute of Biology, State University of Campinas, Campinas, Brazil*
[c] *Department of Biophysics, Federal University of São Paulo, São Paulo, Brazil*
[d] *Department of Experimental Medicine, Sect. Chemistry and Structural Biochemistry, University of Parma, Parma, Italy*

Received 23 January 2006; received in revised form 17 March 2006; accepted 19 March 2006
Available online 27 March 2006

Abstract

The peptide *p*IV/S4–S5 encompasses the cytoplasmic linker between helices S4–S5 in domain IV of the voltage-gated Na^+ channel, residues 1644–1664. [2] The interaction of two local anesthetics (LA), lidocaine and benzocaine, with *p*IV/S4–S5 has been studied by DOSY, heteronuclear NMR ^1H–^{15}N-HSQC spectroscopy and computational methods. DOSY indicates that benzocaine, a neutral ester, exhibits stronger interaction with *p*IV/S4–S5 than lidocaine, a charged amine-amide. Weighted average chemical shifts, $\Delta\delta(^1H–^{15}N)$, show that benzocaine affects residues L^{1653}, M^{1655} and S^{1656} while lidocaine slightly perturbs residues I^{1646}, L^{1649} and A^{1659}, L^{1660}, near the N- and C-terminus, respectively. Computational methods confirmed the stability of the benzocaine binding and the existence of two binding sites for lidocaine. Even considering that the approach of studying the peptide in the presence of a co-solvent (TFE/H_2O, 30%/70% v/v) has an inherently limited implication, our data strongly support the existence of multiple LA binding sites in the IV/S4–S5 linker, as suggested in the literature. In addition, we consider that LA can bind to the S4–S5 linker with diverse binding modes and strength since this linker is part of the receptor for the "inactivation gate particle". Conditions for devising new functional studies, aiming to better understand Na^+ channel functionality as well as the various facets of LA pharmacological activity are proposed in this work.

Keywords: Voltage-gated sodium channel; Peptide; Local anesthetics; Benzocaine; Lidocaine; Nuclear magnetic resonance

1. Introduction

Voltage-gated Na^+ channels are responsible for the initiation and propagation of action potentials in a variety of excitable cells [1–3]. In response to membrane depolarization, the Na^+ channels open and allow the influx of sodium ions into the cells. Sodium channels are concentrated in axons and muscle cells and they have a molecular architecture consisting of α and β subunits. The α-subunit (260 kDa) is composed of four homologous domains (I–IV), each containing six transmembrane helices (S1–S6) [1–3].

During maintained depolarization, the channels switch, in a millisecond time scale, to an inactivated non-conducting state and re-polarization of the membrane is required for its recovery [4]. The fast inactivation gating of the Na^+ channel has been only partly deciphered. The sequence Ile–Phe–Met, the IFM

Abbreviations: BZC, benzocaine; CD, circular dichroism; COSY, correlation spectroscopy; DOSY, diffusion ordered spectroscopy; DSS, 4,4-dimethyl-4-silapentane-1-sulfonate; HSQC, heteronuclear single quantum coherence; LA, local anesthetics; LDC, lidocaine; NMR, nuclear magnetic resonance; NOESY, nuclear Overhauser effect spectroscopy; SDS, sodium dodecyl-sulfate; TFE, trifluoroethanol; TOCSY, total correlation spectroscopy.

* Corresponding authors. E. de Paula is to be contacted at Department of Biochemistry, Institute of Biology, State University of Campinas, Campinas, Brazil, Fax: +55 19 3788 6129. T.A. Pertinhez is to be contacted at Department of Experimental Medicine, University of Parma, Parma, Italy, Fax: +39 0521 903802.

E-mail addresses: depaula@unicamp.br (E. de Paula), thelma@unipr.it (T.A. Pertinhez).

[1] University of Sorocaba, Sorocaba, Brazil (permanent address).

[2] Residues numbering correspond to the primary sequence of the voltage-gated human brain Na^+ channel [1].

0301-4622/$ - see front matter © 2006 Elsevier B.V. All rights reserved.
doi:10.1016/j.bpc.2006.03.010

motif, located in the intracellular linker between domains III and IV, has been identified as the "inactivation gate particle" [5,6] since it participates in the channel pore blocking. However, the residues at the channel intracellular mouth required for the binding of the "inactivation gate particle" and for channel fast inactivation have not yet been positively identified.

The short intracellular loops connecting the S4 and S5 helices, both at domains III [7,8] and IV [9,10], appear to be good candidates for this role. For instance, McPhee and co-workers [10] have shown that residues F^{1651}, L^{1660}, and N^{1662} in the S4–S5 linker of domain IV (IV/S4–S5 linker) establish hydrophobic interactions with the IFM motif during the inactivation of human brain Na^+ channels. In addition, site-directed mutagenesis studies revealed that, in rat skeletal muscle Na^+ channel, substitution of the linker non-polar residues before P^{1473} gives rise to non-functional channels [6,8]; similar results have been observed by Tang and co-workers in the human heart Na^+ channel subtype 1 [9]. Overall, these results point to a direct involvement of the IV/S4–S5 linker in channel inactivation.

Filatov and co-workers [6] also suggested that the non-polar surface of the S4–S5 helices of rat skeletal muscle sodium channel interacts with the non-polar surface of helices of adjacent domains in response to conformational changes associated with channel activation [11,12] and this movement would contribute to the formation of a binding site for the "inactivation gate particle", i.e., the so-called "inactivation gate receptor" [6]. Specific residues of the S6 helix of domains I and II [13] and IV [14] have also been found to interact with the "inactivation gate particle". In an interesting manner, these helices, in conjunction with S5 helices of each segment, line the inner part of the channel pore [14]. Taken together, these results suggest that the formation of the "inactivation gate receptor" is the result of a conformational re-arrangement involving at least the S6 helices and the IV/S4–S5 linker [10,14,15].

LA act by binding to the Na^+ channel, inhibiting Na^+ uptake and blocking the nervous impulse. Many LA are ionizable amines and both the charged and uncharged forms are now considered relevant for the mechanism of anesthesia. In the past, it has been proposed that while the uncharged form is ideal to cross the cell membrane, the binding to a specific site on the channel would be achieved by the protonated species [16,17] only in the intracellular side. Nevertheless, this hypothesis has always been questioned since benzocaine (BZC), the only clinically used local anesthetic that is neutral at physiological pH, produces tonic inhibition of Na^+ channels, with little dose-dependent blockade during repetitive depolarization. Interestingly, other hydrophobic analogues of BZC elicit a dose-dependent blockade of the channel [18,19]. In addition, BZC binding, as well as the binding of charged tertiary and quaternary amine LA, seems to be channel-state-dependent, being favored when the channel is in its open or inactivated state [14,20].

Along the years, much work has been devoted to describe the molecular mechanism associated to LA pharmacological activity [13,21,22,23]. The first mapping of LA binding sites in Na^+ channels revealed that three residues (I^{1760}, F^{1764}, Y^{1771} of rat skeletal muscle μ1), in the middle of helix IV/S6, are critical for the uncharged anesthetic species binding [23,24]. Further studies suggested that, particularly when Na^+ channels are in their inactivated state, one additional residue (I^{409}) in the middle of helix I/S6 is aligned in close proximity to the tertiary amine moiety of amino-amide LA [25,26]. Recently, Godwin and co-workers [19] constructed, in silico, a structural model for the binding of BZC to the IV/S6 helix of the same Na^+ channels of rat skeletal muscle. The model proposes that four hydrophobic residues (V^{1582}, M^{1585}, I^{1581} and I^{1589}) form an ideal binding cavity for neutral LA where, in fact, the benzenoid ring of BZC can be docked. Interestingly, since bulkier BZC analogues (ethyl-4-ethoxy and ethyl-4-diethylamino benzoates) are characterized by a higher association constant and best fit that binding site, the authors suggest this might be the explanation for the dose-dependent blockade observed for those analogues and not for BZC [18,19]. Although the authors have analyzed only the IV/S6 helix, a critical and well-known LA binding site [23,27,28], they hypothesize, based on the ideas described in the classical review by Hille [20], that other regions in the Na^+ channel α-subunit ought to be considered as LA potential binding sites. Those regions could include hydrophobic residues of the III–IV linker, the "inactivation gate particle" [23], residues close to a proline in the S5–S6 linker of domains I and IV, which control the ion selectivity of Na^+ channels [29] and the S4–S5 intracellular linker of domain IV that is part of the "inactivating gate receptor" [6,8–10,14,22].

Miyamoto and co-workers [30] have determined the structure, in SDS micelles, of a peptide encompassing a portion of the IV/S4–S5 linker of the human brain Na^+ channel: Ac-TLLFALMMSLPALFNIGLL-NH_2, residues 1648–1666. In partial agreement with a previous secondary structure prediction [6], the study shows that the peptide presents a hydrophobic α-

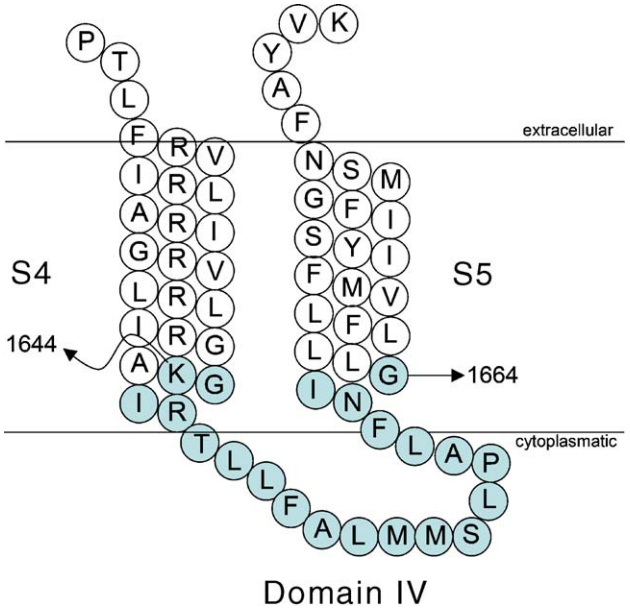

Fig. 1. Model of the cytoplasmic linker connecting helices S4–S5 of domain IV of the α-subunit of adult human brain Na^+ channel. The sequence of the peptide *p*IV/S4–S5 studied in this work is colored in gray.

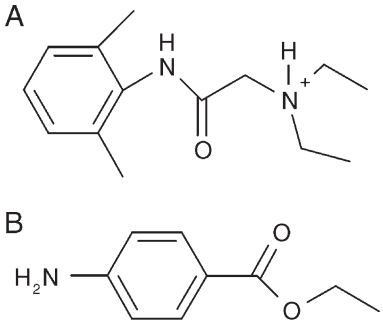

Fig. 2. Chemical structure of LA used in this study: A) lidocaine (LDC); B) benzocaine (BZC).

helical region encompassing residues L^{1650}–S^{1656} and a β-turn after P^{1658}. Moreover, the authors suggest that the binding of the "inactivation gate particle" to the "inactivation gate receptor" would require the interaction of the residues $IFM^{1488–1490}$, $YY^{1497–1498}$ and M^{1501} of the "inactivation gate particle" with the residues F^{1651}, $MM^{1654–1655}$, L^{1657} and A^{1659} located in the IV/S4–S5 linker, respectively.

Since most of the experimental data collected so far point to the IV/S4–S5 linker as a potential region for LA binding, using NMR Diffusion Ordered Spectroscopy (DOSY), $^{1}H–^{15}N$ HSQC experiments and computational methods, we have studied the interaction of the synthetic peptide *p*IV/S4–S5 with the local anesthetics LDC and BZC. The *p*IV/S4–S5 (KGIRTLLFALMMSLPALFNIG-NH_2, 1644–1664) encompasses the entire IV/S4–S5 linker (Fig. 1) of the human brain voltage-gated Na^+ channel. LDC is an amine-amide local anesthetic that, although at physiological pH exists as positively charged and uncharged species, in our experimental conditions is fully charged (Fig. 2A) while BZC is a local anesthetic that is always uncharged both at physiological pH and in our experimental conditions (Fig. 2B).

2. Experimental

LDC and BZC have been obtained from Sigma Chemical Co (St. Louis, MO). All other reagents were of analytical grade.

2.1. Peptide synthesis and purification

The peptide: KGIRTLLFALMMSLPALFNIG-NH_2 (*p*IV/S4–S5) was synthesized manually, according to the standard t-Boc/Bzl strategy [31,32]. *p*-methylbenzhydrylamine-resin (0.79 mmol/g) was used as the solid support and the following side-chain protecting groups were used: 2-Cl-benzyloxycarbonyl (Lys), *p*-toluenosulphonyl (Arg) and benzyl (Thr and Ser). The α-amino-group de-protection and neutralization steps were performed in 30% (v/v) trifluoroacetic acid/dichloromethane for 30 min and in 10% (v/v) *N*,*N*-diisopropylethylamine/dichloromethane for 10 min. The coupling reaction was carried out with the acylating agents 2-(benzotriazol-1-yl)-1,1,3,3-tetramethyluronium tetrafluoroborate/N_1-hydroxybenztriazole/*N*,*N*-diisopropyl ethylamine in a three fold excess condition over the amount of resin-bound amine groups. Cleavage of peptide from the resin was performed in fluoridric acid/*o*-cresol/dimethylsulfide (9.0/0.5/0.5 v/v/v) at 0 °C, for 90 min. The resin was rinsed with ethyl acetate and the peptide was extracted with 5% acetic acid and then, lyophilized.

Peptide purification was carried out using a Waters 510 HPLC instrument with a Vydac C_{18} semi-preparative column, using 0.1% trifluoroacetic acid/H_2O as solvent A and 0.08% TFA/60% acetonitrile (ACN)/H_2O, as solvent B.

A linear gradient of solvent B ranging from 25% to 65% was applied over a period of 2 h. The homogeneity and purity of the peptide was characterized by analytical HPLC (Waters), electro spray LC/MS mass spectrometry (Micromass) and amino acid analysis (Biochrom 20 Plus, Amersham-Biosciences); the measured mass was m/z 2307 (calculated 2306.90).

2.2. Circular dichroism experiments

Circular dichroism measurements were carried out on a Jasco J-810 spectropolarimeter equipped with a Peltier Jasco PFD-425S system for temperature control. The far UV-CD spectra were acquired in the spectral range of 190–250 nm at 25 °C, using quartz cells of 1 or 2 mm path length. Four scans were averaged for each experiment and the blank spectra were subtracted. The optical activity is reported as the mean residue molar ellipticity, θ (deg cm^2 $dmol^{-1}$).

The samples were prepared by dissolving the lyophilized peptide either in pure water, in SDS or in TFE water mixtures to a final peptide concentration of 50 μM. The pH was adjusted to 7.4 by adding small aliquots of NaOH and HCl unless otherwise indicated.

2.3. NMR experiments

The sample for the structure determination was prepared by dissolving the peptide in 30%/70% v/v TFE/H_2O mixture to yield a concentration of 1.0 mM, at pH 4.0. The ^{1}H NMR experiments were carried out on a Varian Inova 600AS spectrometer operating at 599.68 MHz for ^{1}H, at 25 °C. The spectral width was typically 8000 Hz and, 648 τ_1 increments were recorded with 64 transients of 2K complex points for each free induction decay. The proton chemical shifts were referenced to 4,4-dimethyl-4-silapentane-1-sulfonate, DSS (0.00 ppm). The peptide ^{1}H sequential assignment was achieved by standard procedures [33]. The spin systems of the individual amino acid residues were unequivocally identified from COSY [34], TOCSY [35] with 85 ms mixing time and NOESY [36] with 200 and 400 ms mixing times, experiments. For the ^{15}N chemical shifts assignment, natural abundance $^{1}H–^{15}N$ HSQC spectra were acquired using 128 increments and 32 transients with 1 K of complex points. The spectral width was 2200 Hz and 6000 Hz for ^{15}N e ^{1}H dimensions, respectively.

Data were processed on a workstation Silicon Graphics Octane2, using the FELIX NMR 2000 Software (Accelrys Inc., San Diego, CA). Prior to Fourier transformation, the time domain data were zero-filled in both dimensions in order to yield an 8 K × 2 K data matrix. When necessary, a fifth-order

polynomial baseline correction was applied after transformation and phasing.

In order to obtain the inter-proton distances, cross-peaks volumes from the 200 ms NOESY spectrum were calibrated with respect to the cross-peak volume of the well-defined geminal β-protons, which corresponds to the distance of 1.8 Å. The resulting inter-proton distance constraints were classified as strong (1.8–2.5 Å), medium (1.8–3.5 Å) and weak (1.8–5.0 Å). Upper distance restraints, involving non-stereo-specific assigned methylene, aromatic and methyl protons were replaced by appropriated pseudo-atoms [32].

Aiming to investigate the interaction between LA and the *p*IV/S4–S5 peptide, LDC and BZC were added directly to the peptide solution, 1 mM, to reach the desired anesthetic: *p*IV/S4–S5 molar ratio for each experiment (molar ratios from 1:4 up to 5:1). $^{1}H–^{15}N$ HSQC and DOSY experiments were carried out on a Varian Inova 500AS spectrometer operating at 499.78 MHz for ^{1}H, at 25 °C. The $^{1}H–^{15}N$ HSQC spectra were collected in the presence of increasing anesthetic:*p*IV/S4–S5 molar ratios: 0.25, 0.50, 0.75, 1.00, 2.00 and 5.00 in natural abundance. Weighted average chemical shifts were calculated according to the formula $\Delta\delta(^{1}H,^{15}N)=|\Delta\delta(^{1}H)|+0.2*|\Delta\delta(^{15}N)|$, as described elsewhere [37].

The DOSY experiments were carried out using the BPPSTE (bipolar pulse pairs stimulated echo) method [38]. The duration of the total diffusion-phase encoding gradient pulse was 2 ms, the diffusion delay was 0.05 sec and the minimum gradient strength was set to 0.3 Gauss/cm. The diffusion coefficients were measured in the absence and presence of LA, at a 1:1 LA: *p*IV/S4–S5 molar ratio.

2.4. DOSY data analysis

For both LA, the peptide bound fraction was measured as previously described [38,39]. Assuming that bound and free LA undergo fast exchange in the diffusion time scale, the observed LA diffusion coefficient, $D_{free+bound}$, is the weighted average of the unbound, D_{free}, and *p*IV/S4–S5-bound, D_{bound}, values (Eq. (1)).

$$D_{free+bound} = (1 - f_{bound})D_{free} + f_{bound}D_{bound} \quad (1)$$

where f_{free} and f_{bound} are the fractions of free anesthetic and LA bound to *p*IV/S4–S5, respectively, and $f_{free}+f_{bound}=1$. D_{free} is the diffusion coefficient of the unbound anesthetic and D_{bound} is the one of the *p*IV/S4–S5/anesthetic complex. Rearrangement of Eq. (1) gives:

$$f_{bound} = (D_{free} - D_{free+bound})(D_{free} - D_{bound})^{-1}. \quad (2)$$

Recognizing that LA molecular size are much smaller than the one of *p*IV/S4–S5, we assumed, as already suggested by other authors [38], that the diffusion coefficient of the anesthetic bound to the peptide corresponds to the one of the *p*IV/S4–S5 alone.

2.5. Computational methods

2.5.1. NMR-derived peptide structure

The NMR-derived 3D structure of the peptide was determined using DYANA [40]. Each round of refinement started with 20 random conformers. The 10 lowest target function models were used to analyze constraint violations and to assign additional NOE constraints to be included in the subsequent calculation. This process was repeated until all violations were eliminated. In the final refinement round, a total of a hundred structures were calculated and the 40 conformers presenting the lowest target function were considered for further analysis. After simulated annealing, the 40 structures, characterized by a target function smaller than 1.0 $Å^2$ and by distance violation no larger than 0.2 Å, were energy minimized in the Consistent Valence Force Field (Morse and Lennard-Jones potentials, coulombic term) by steepest descents and conjugated gradients, using several thousands interactions, until the maximum derivative was less than 0.001 kcal/Å. All calculations were carried out on a Silicon Graphics Octane2 workstation, using the DISCOVER (Accelrys, Inc., San Diego, CA) software implemented in the INSIGHT II package.

The quality of the final structures was analyzed on the basis of the root mean square deviation (r.m.s.d.) and by the PROCHECK-NMR program [41].

2.5.2. Docking and MD calculations

Docking and molecular visualization procedures were performed using the INSIGHT II graphical environment on a Silicon Graphics Octane2 workstation. The MD calculations and trajectory analysis were carried out using the GROMACS suite of programs [42] running on a Compaq AlphaServer ES40 multiprocessor.

2.5.2.1. Docking. BZC and LDC were built and energy optimized with the Biopolymer and Discover modules of INSIGHT II. The starting locations of the LA docked to the NMR-derived minimum energy structure of *p*IV/S4–S5 were obtained using as a guide the $\Delta\delta(^{1}H,^{15}N)$ experimentally observed, measured for the *p*IV/S4–S5 residues in the presence of BZC and LDC, respectively. Subsequently, the complexes were optimized in order to cancel the steric hindrance and minimum energy of the resulting complex.

2.5.2.2. MD simulation system set up. As explained in the Results and discussion section, the finding of two distinct binding sites for LDC prevented us from carrying out the MD simulation of this system. Instead, this was possible for BZC. The energy minimized complex formed by BZC bound to *p*IV/S4–S5 was immersed in a triclinic box filled with a mixture of simple point charge (SPC) water molecules [43] and TFE model [44] molecules, corresponding to approximately 30%/70% v/v TFE/H_2O mixture and resulting in a system composed by 96 TFE plus 1658 H_2O molecules. The box size was adjusted in a way to assure a minimum distance of 0.8 nm between the complex and the edges of the periodic box. The net charge of the

system (+3) was neutralized with the correspondent number of Cl^- counterions.

2.5.2.3. MD simulation parameters. The calculations were performed using the GROMOS96 force field [45]. The system was simulated using periodic boundary conditions with a cut-off radius of 0.8 nm for short-range interactions, being the neighbor pair list updated at each 10 steps. Long-range electrostatics interactions were treated with the Particle Mesh Ewald method [46,47]. The LINCS algorithm [48] was used to constrain all bond lengths and SETTLE [49] to constrain water geometries. A time step of 2 fs was chosen for integrating the equations of motion. Since the NMR experiments have been carried out at standard laboratory conditions, the MD simulation has been performed at constant temperature (298 K) and pressure (1 bar).

2.5.2.4. Simulation protocol. The solvated *p*IV/S4–S5: BZC complex was submitted to an initial relaxation of solvent and ions through 500 steps of the steepest descent energy minimization algorithm, while keeping the peptide coordinates fixed. The system was then submitted to another short minimization step with a backbone position restraints applied with a force constant of 1.000 kJ/mol/nm^2. Thereafter, the system was submitted to a 3 ns molecular dynamics (MD) simulation. During this final MD simulation time, the structures of the complex were collected every 1 ps.

3. Results and discussion

3.1. Searching for the ideal conditions to study LA: pIV/S4–S5 interaction

The CD spectra of the peptide in water did not reveal any dependence on peptide concentration (data not shown). In contrast, as demonstrated by previous studies [30,50], the peptide turned out to be characterized by a high conformational plasticity, being sensitive to variations in the experimental conditions such as ionic strength, nature of the salts and temperature. In fact, by varying those parameters, *p*IV/S4–S5 undergoes conformational transitions from a random coil conformation to a helical coiled-coil structure or to some other type of more aggregated state (data not shown). Due to the high sensitivity to ionic strength and ions nature, we have not been able to describe, in a reliable manner, its conformational pH dependence.

Fig. 3 shows the CD spectrum of the peptide in water, at pH 7.4. The negative band at 203 nm is reminiscent of a peptide in random coil conformation; nonetheless the presence of the weak negative band in the region 220–225 nm suggests the presence of some helical elements. Indeed, the analysis of the spectrum according to Gans and co-workers [51] indicates that the helix content, in these experimental conditions, is 14%. Considering the fact that the peptide has an amino acid composition and an hydrophobicity typical of a transmembrane helix and since this region of the Na^+ channel is expected to be internalized when the channel is in the open state, we have tested the peptide in the presence of either the co-solvent TFE and SDS micelles, two mimetics of a lipid membrane environment, Fig. 3. The shift of the negative band from 203 nm to 208 nm and the concomitant intensity increase of both the negative and the positive band (222 nm and 196 nm, respectively) clearly indicate an increase of α-helix secondary structure. The TFE titration, as shown by the intensity variation of the 220 nm band, Fig. 3—inset, demonstrates that the helical content stabilizes above 15% TFE. The analysis of these spectra according to [51] indicates that, in TFE, the peptide acquires a maximum α-helix content of 43%. A similar behavior is observed with SDS micelles (data not shown)—in the presence of 20 mM SDS, Fig. 3, the α-helical

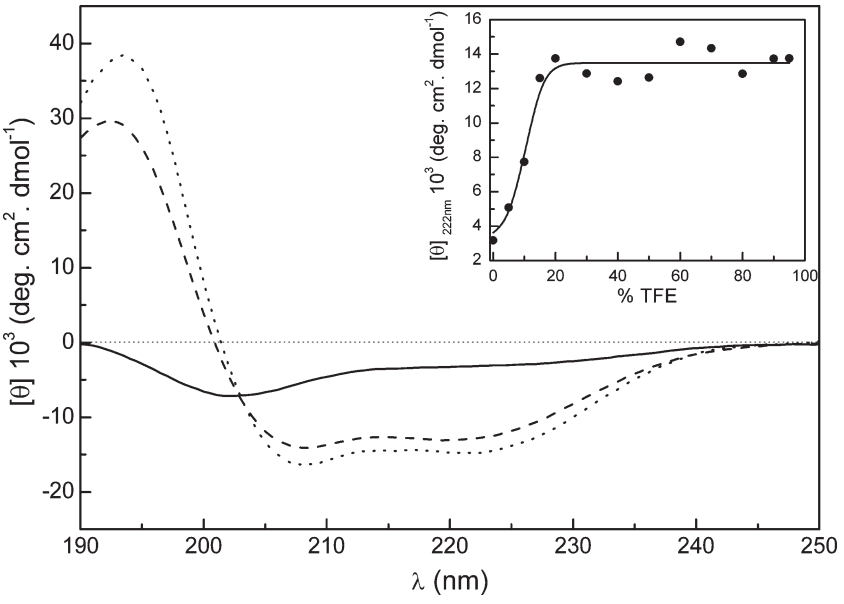

Fig. 3. Far-UV CD spectra of pIV/S4–S5 (50 μM) in water, pH 7.4 (solid line), in 30%/70% v/v TFE/H_2O mixture pH 4.0 (dashed-line) and in the presence of 20 mM SDS pH 7.4 (dotted-line). The inset shows the TFE-induced conformational transitions of *p*IV/S4–S5, pH 4.0 at 25 °C followed by means of $[\theta]_{222}$. All measurements have been carried out at 25 °C.

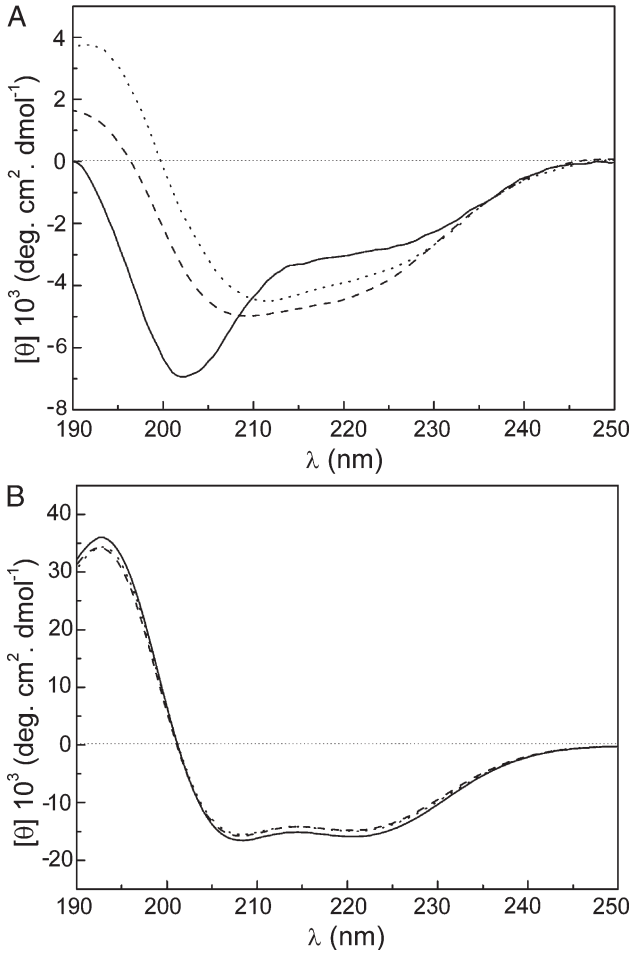

Fig. 4. Far-UV CD spectra of *p*IV/S4–S5 (50 μM) A) in water, pH 7.4 (solid line), in the presence of: BZC 50 μM (dashed line) and 400 μM (dotted line) B) in 30%/70% v/v TFE/H_2O mixture, pH 4.0, in the presence of: BZC 50 μM (solid-line) and 400 μM (dotted-line) at 25 °C.

content reaches its maximum of 47%. The tendency of *p*IV/S4–S5 to acquire an α-helical fold has been confirmed by the fact that the peptide displayed the same secondary structure also in other organic solvents such as methanol and acetonitrile (data not shown).

CD experiments were also carried out with the peptide dissolved in water or in TFE/water mixtures and in the presence of variable amounts of LA. Distinct responses were observed depending on the medium used. As an example, Fig. 4A shows the effect of several concentrations of BZC on the peptide dissolved in water, at pH 7.4. It is possible to assert that the induction of elements of secondary structure depends on the LA concentration. The increasing red shift of the CD spectra cross-over is indicative of the onset of some sort of aggregation.

Fig. 4B reports the CD profiles of the peptide dissolved in 30%/70% v/v TFE/H_2O mixture, pH 4.0, upon addition of BZC. Once we verified that in these experimental conditions the peptide CD spectra are not modified by pH variations, we have used pH 4.0 considering the fact that NMR experiments are better carried out in that pH value. In this case, it is possible to observe only a slight, though significant, change in the spectrum intensity while the CD profile is not modified, thus suggesting that LA do interact with the peptide without inducing any aggregation effect. In these conditions, the binding is expected to produce only distortions of the helical fold and not major conformational transitions, thus justifying the observed spectroscopic changes. A similar general behavior is also observed when the peptide interacts with LDC (data not shown).

3.2. The NMR-derived solution structure of pIV/S4–S5

We have determined the peptide 3D solution structure in 30%/70% v/v TFE/H_2O mixture based on the following considerations derived from the CD experiments: a) anesthetic: IV/S4–S5 interaction in water induces the peptide to acquire some sort of helical conformation. In addition, we know that LA present a preferential binding to the open or inactivated [20] rather than to the closed channel state, i.e., when the peptide is structured. Thus it is conceivable to assume that the helical fold acquired by the peptides in 30%/70% v/v TFE/H_2O mixture is compatible with the presence of LA binding sites. b) The peptide possesses similar helical secondary structure in both TFE/water mixtures and in the presence of SDS micelles. c) Being interested in highlighting the possible existence of LA binding sites, we privileged a solvent that could leave the peptide surface fully accessible to the potential ligands. d) In these experimental conditions, while the peptide acquire a conformation already exhibiting the potential LA binding sites, we avoid the onset of aggregation processes that might impair the possibility to identify the selected amino acids involved in the interaction with the anesthetic.

The ^1H NMR resonance assignment has been carried out based on the combined use of two-dimensional TOCSY and NOESY spectra [33]. The *p*IV/S4–S5 ^1H and ^{15}N chemical shifts have been deposited in the BioMagResBank (accession number 5837).

Fig. 5 summarizes the short and medium range NOEs. The dense pattern of $d_{\alpha N}(i,i+3)$, $d_{\alpha N}(i,i+4)$ and $d_{\alpha\beta}(i,i+3)$ indicates that the helix extends between residues G^{1645} and I^{1663} and the fact that the $d_{NN}(i,i+1)$ are stronger than the $d_{\alpha N}(i,i+1)$ suggests the helix is rather stable.

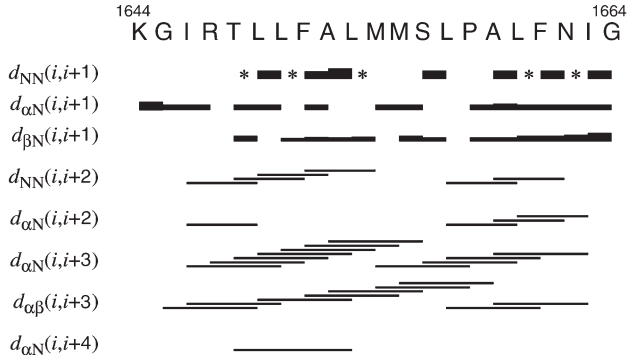

Fig. 5. Summary of the sequential and medium-range NOE connectivities for *p*IV/S4–S5 (1.0 mM) in 30%/70% v/v TFE/H_2O mixture, at pH 4.0 and 25 °C. The intensities of the observed NOE are represented by the thickness of lines and were classified as strong, medium and weak, corresponding to upper bound constraints of 2.5, 3.5 and 5.0 Å, respectively. The stars indicate potential NOE connectivities that could not be obtained due to resonance overlap.

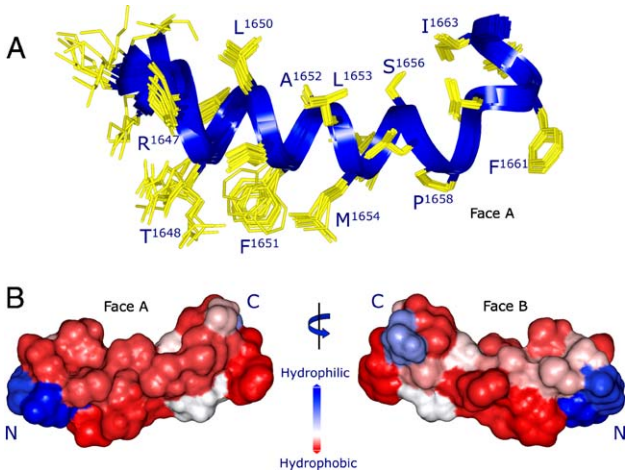

Fig. 6. A) Ensemble of the 20 final structures of *p*IV/S4–S5 with superposition over residues I^{1646} to N^{1662}. B) Hydrophobic potentials surface of *p*IV/S4–S5 with calculated using InsightII. Hydrophobic and hydrophilic surfaces are shown in red and blue, respectively, whereas white represents an intermediary hydrophobicity. (For interpretation of the references to colour in this figure legend, the reader is referred to the web version of this article.)

Fig. 6A displays the superposition of the best 20 models, selected on the basis of their minimum energy and of the residual distance violation less than 0.2 Å. The quality of the structures has been evaluated using PROCHECK-NMR [41] and it is reported in Table 1. As it can be seen, 95% of ϕ and ψ angles are in the most favored region with the remaining 5% in the favored region (Table 1). In the region I^{1646}–N^{1662} the peptide acquires a well-defined hydrophobic helical structure, Fig. 6A, as indicated also by the low r.m.s.d., Table 1. A bend is present at residue P^{1658}, Fig. 6A. All side chains are characterized by a well-defined spatial organization.

It is worth noting that our structure is somewhat different from the one reported for the peptide Ac-TLLFALMMSL-PALFNIGLL-NH_2 (residues 1648–1666) in SDS micelles [30]. In fact, in that case a β-turn is detected subsequent to the proline residue. This apparent discrepancy may be justified by the fact that, in SDS micelles, the C-terminal portion of the peptide is likely to be located near the negatively charged micelle surface, an environment less favorable for α-helix conformation. On the other hand, if we consider a previous secondary structure prediction for this peptide in the homologous rat skeletal muscle sodium channel [6], we find that not only the experimental structures confirm the existence of an helix spanning from the N-terminus to P^{1658} and a bend at that proline residue, but they also show that the helix is hydrophobic and not amphipathic, Fig. 6B. As for the discrepancy in C-terminus it may indicate the existence of conformational freedom in that region.

Table 1
Structure statistics for the ensemble of the 20 minimum energy NMR-derived structures of *p*IV/S4–S5 in 30%/70% v/v TFE/H_2O mixture, pH 4.0 at 25 °C

Constrains	
Intraresidue	102
Sequential	32
Medium range	65
Total	199
PROCHECK analysis	
Most favored region (%)	95%
Additionally allowed region (%)	5%
r.m.s.d. [a]	
Backbone (residues K^{1644}–G^{1664})	0.55±0.26
Heavy atoms (residues K^{1644}–G^{1664})	1.15±0.45
Backbone (residues I^{1646}–N^{1662})	0.12±0.04
Heavy atoms (residues I^{1646}–N^{1662})	0.70±0.02

[a] Root mean square deviation from pairwise comparison between all the structures (Å).

3.3. Interaction of LA with pIV/S4–S5

3.3.1. NMR results

LA are molecules that reversibly block the action potential in excitable membranes [52] by binding to the Na^+ channel and stabilizing it in the inactivated state [8,20,53]. The linker between helices S4 and S5 in domain IV is involved in the stabilization of the inactivated state and it has been indicated as a putative site of action for LA [10,14,22,54].

In order to verify the existence of specific interactions between each local anesthetic and *p*IV/S4–S5, a series of ^1H–^{15}N HSQC experiments in which the peptide was mixed with increasing concentrations of either LDC or BZC corresponding to LA:*p*IV/S4–S5 molar ratios of 0.25, 0.50, 0.75, 1.0 and 5.0, were carried out. The perturbation induced by the LA reaches a plateau at a 1:1 LA:*p*IV/S4–S5 molar ratio (data not shown).

Aiming to obtain more insights on the binding of LA to the peptide, we performed DOSY experiments. The analysis of the NMR-derived diffusion coefficients, Table 2, confirmed that both LA interact with *p*IV/S4–S5 and that, in the experimental conditions tested, 35% of the BZC molecules bind to the peptide, while the percentage drops to 13% for LDC.

Several authors have proposed the use of changes in chemical shifts as an efficient way for structure-based drug discovery and design [55,56]. In particular, it has been suggested that the weighted-average chemical shifts, $\Delta\delta(^1H,^{15}N)$, is the most effective way to identify the contacts between a ligand and a protein [37]. Fig. 7 describes the results obtained at 1:1 LA:*p*IV/S4–S5 molar ratio. Despite a slight diffuse variation of $\Delta\delta(^1H,^{15}N)$, suggesting that LA are indeed in the peptide vicinity, we measured relatively higher values for

Table 2
LA and *p*IV/S4–S5 diffusion constants (10^{-10} m^2 s^{-1}) and percentage of each LA bound to the peptide

Local anesthetic	D_{free}	D_{bound}	$D_{free+bound}$	$f_{bound\ (\%)}$
LDC	2.92±0.138	1.08±0.192	2.68±0.174	13
BZC	2.87±0.199	1.08±0.165	2.24±0.129	35

D_{free}=diffusion coefficient of the free LA; D_{bound}=diffusion coefficient of the complex (see Section 2); $D_{free+bound}$=diffusion coefficient of both bound and free LA, 1:1 LA:*p*IV/S4–S5, molar ratio, 30%/70% v/v TFE/H_2O mixture, pH 4.0 at 25 °C. $f_{bound\ (\%)}$: percentage of LA bound calculated as described in Section 2 [38,39].

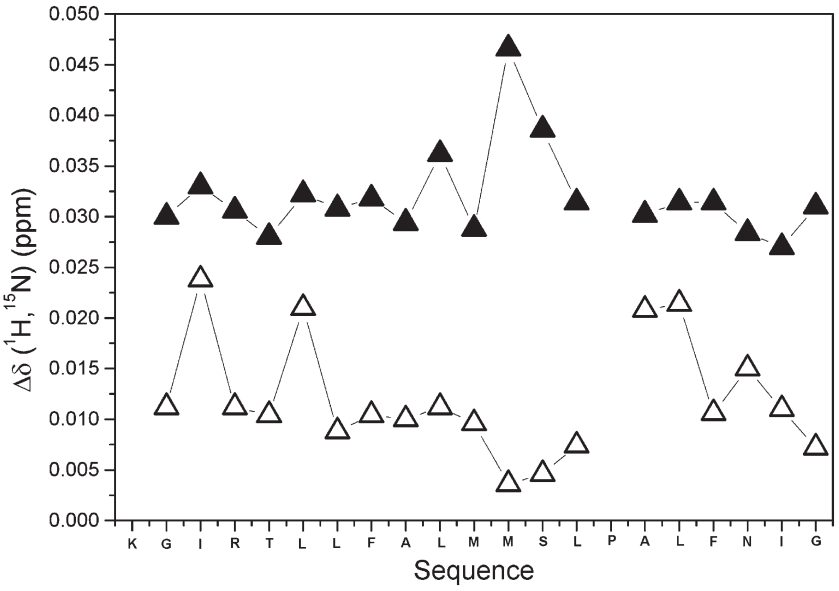

Fig. 7. Weighted averaged chemical shifts $\Delta\delta(^1H,^{15}N)$, [38], of *p*IV/S4–S5 backbone NHs in the presence of BZC (▲) and LDC (△). *p*IV:S4–S5/LA, 1:1 molar ratio. For details see Section 2.

few selected residues. The fact that BZC induces a more intense perturbation than LDC supports the DOSY data, proposing a higher percentage of binding for BZC.

Therefore, our data not only demonstrate that the two LA interact with diverse intensity with *p*IV/S4–S5, but also reveal that they have various preferential contacts: BZC interacts with L^{1653}, M^{1655} and S^{1656}, while LDC interacts with I^{1646}, L^{1650}, A^{1659} and L^{1660}, Fig. 7.

3.3.2. Computational analysis

Based on the analyses of Fig. 7, we have used molecular modeling to identify the models that might better represent BZC and LDC bound to the peptide, respectively.

Fig. 8A shows the result of the BZC docking to *p*IV/S4–S5. The three residues (L^{1653}, M^{1655} and S^{1656}) indicated by the NMR experiments to be preferentially affected by the presence of BZC are represented in orange. Fig. 8B,C depicts the two possible modes of LDC binding. The orientation of the anesthetic molecule has been initially guided by the NMR results and then it has been refined based both on the minimum steric hindrance and minimum energy of the obtained complexes. Interestingly, in agreement with the NMR data, the minimum energy of BZC docked to the peptide turns out to be much lower than the one obtained for the LDC: *p*IV/S4–S5 complexes, Table 3. In general, the models suggest that the predominant hydrophobic character of the helical surface of *p*IV/S4–S5, Fig. 6B, may justify the preferential affinity for uncharged molecules, as also suggested by previous results [57,58].

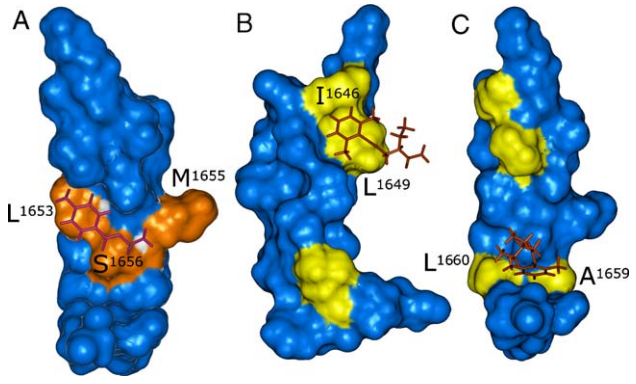

Fig. 8. Docking on the peptide *p*IV/S4–S5 of: A) BZC; B) LDC bound to site 1; C) LDC bound to site 2. The peptide is presented by its solvent accessible surface and the peptide residues interacting with LA are colored: A) L^{1653}, M^{1655} and S^{1656} (orange); B, C) I^{1646}, L^{1649}, A^{1659} and L^{1660} (yellow). C-terminus is at the bottom. For sake of clarity in Panels B) and C) the peptide is represented in two different orientations. (For interpretation of the references to colour in this figure legend, the reader is referred to the web version of this article.)

To validate the quality of the docking, we carried out a 3ns MD simulation of the BZC:*p*IV/S4–S5 complex in the same 30%/70% v/v TFE/H_2O mixture in which the NMR experiments have been carried out. We did not test LDC due to the complexity derived by the occurrence of two biding sites and it is not possible to know, analyzing the experimental results, if one or two molecules of LDC bind at a time.

Table 3
Intermolecular interaction energies characterizing the complexes obtained from the docking of BZC and of LDC on peptide *p*IV/S4–S5

Local anesthetic	Interaction energies[a] (kcal mol^{-1})		
	vdW	Electrostatic	Total
BZC[b]	−11.689	0.796	−10.894
LDC-1[b]	−5.496	−0.160	−5.656
LDC-2[b]	−2.087	−0.391	−2.477

[a] Interaction energies have been calculated using: vdW = van der Waals energy and Electrostatic = electrostatic energy.

[b] Energetic parameter referring to: docking of BZC to its binding site identified in residues L^{1653}, M^{1655}, and S^{1656} as suggested by the NMR $\Delta\delta$ ($^1H,^{15}N$) results, Fig. 8A; docking of LDC to its binding site 1 identified in residues I^{1646}, L^{1650}, as suggested by the NMR $\Delta\delta(^1H,^{15}N)$ results; Fig. 8B; docking of LDC to its binding site 2 identified in residues A^{1659}, L^{1660}, as suggested by the NMR $\Delta\delta(^1H,^{15}N)$ results; Fig. 8C.

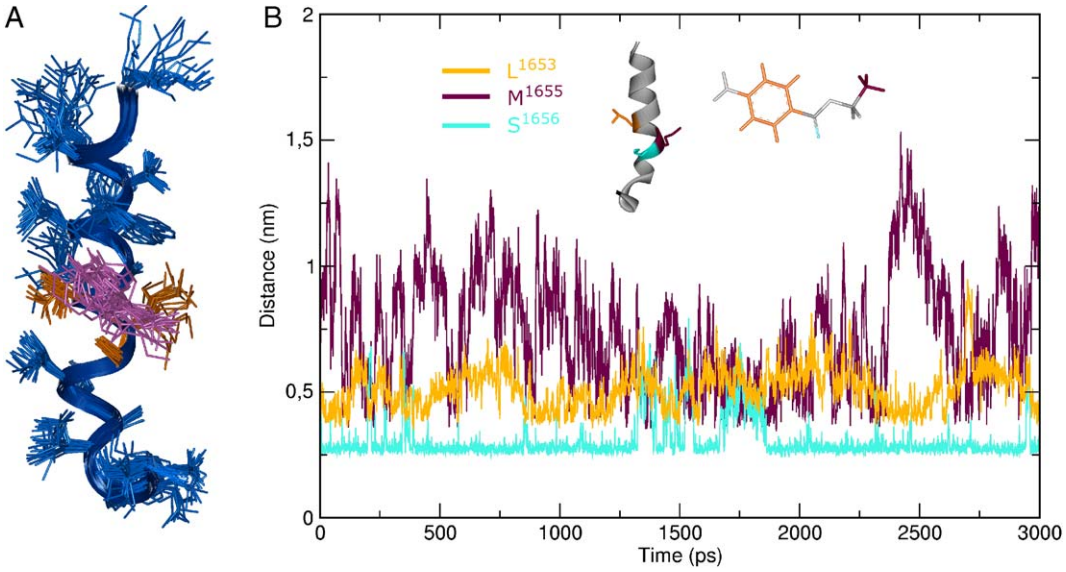

Fig. 9. A) Superposition of 20 docked models of the *p*IV/S4–S5:BZC complex collected along the 3 ns MD simulation with contact atoms highlighted according to the color scheme used in B. B) Monitoring of specific contacts between *p*IV/S4–S5 and BZC during the MD simulation. Distance between the center of mass of the BZC aromatic ring (orange) and the center of mass of L^{1653} side chain (Cγ, Cδ1 and Cδ2); distance between the carbon of the BZC methyl group (violet) and M^{1655} Cε atom; distance between the BZC central carbonyl oxygen (cyan) and the hydroxyl oxygen of the S^{1656} side chain. The one-letter symbols amino acids are colored to match the BZC regions of interaction. (For interpretation of the references to colour in this figure legend, the reader is referred to the web version of this article.)

Fig. 9A shows the superposition of 20 models of the BZC: *p*IV/S4–S5 complex collected along the 3 ns of MD. As it can be seen, BZC fluctuates around the position of the original docking with minimal deviations. Fig. 9B reports the distance of three specific groups of BZC (the aromatic ring, the central carbonyl group and the terminal methyl group) with respect to the center of mass of L^{1653} side chain (Cγ, Cδ1 and Cδ2), to the hydroxyl oxygen of the S^{1656} side chain and to the M^{1655} Cε, respectively. Remarkably, the data reveal the formation of an H-bond involving the BZC central carbonyl group and the S^{1656} OH group that contributes to stabilize the position of BZC regarding S^{1656} and L^{1653}, as seen by the behavior of the corresponding intermolecular distances, Fig. 9B.

Briefly, the MD simulation calculations confirm the quality of the docking and, in addition, highlight the formation of a stable H-bond.

As for LDC, the fact the DOSY and $^{1}H–^{15}N$ HSQC experiments indicate a reduced binding to the peptide might be interpreted either as a sign of lower affinity (since LDC unbinds from the channels much more rapidly than do other, more hydrophobic LA, such as bupivacaine) [14] or as the result of the existence of two binding sites between which the molecule is exchanging. The lower affinity of LDC, relatively to BZC, is supported by the fact that only the charged LDC species is present at the NMR experimental condition (pH 4.0). The existence of different binding sites agrees with the recent report of Leuwer and coworkers [53] that, using electrophysiology measurements in HEK 293–a heterologously expressed human skeletal muscle sodium channel–described the Na^+ channel inactivation caused by lidocaine as a cooperative, Hill-type, effect. Those authors proposed that either there are multiple binding sites for LDC in the channel fast-inactivated state or that lidocaine functions as an allosteric gating effector [61] strengthening the latch mechanism of inactivation. Zamponi and French have also suggested the existence of different sites for LDC after they found out that diethylamide and phenol, which resemble the hydrophilic tertiary amine head and the hydrophobic aromatic portion of the lidocaine molecule, respectively, mimicked the fast and slow inactivation induced by LDC on bovine cardiac and rat skeletal muscle sodium channels [22].

4. Conclusions

In the transition of the voltage-gated Na^+ channel to the open state, the upward movement of helix S4 causes the internalization of a number of IV/S4–S5 linker residues [59]. Moreover, the IV/S4–S5 linker [10] is believed to form, together with the III/S4–S5 linker [7,15] and I, II [13] and IV [14] S6 transmembrane helices, the so-called "inactivation gate receptor". This multi-domains complex structure is formed only when conformational changes in the channel take place during activation and it acts as a binding site for the "inactivation gate particle" [60], thus favoring subsequent channel closure.

In the frame of this model, LA are believed to interact with the "inactivation gate receptor" [54], stabilizing this otherwise transient receptor, keeping the Na^+ channel in its inactivated state and hence producing anesthesia. This model is also in agreement with the idea that LA interact with the inactivated channel [61,62], where the "inactivation gate receptor" still exists but not in the resting state, in which this transient receptor vanishes.

So far, the hypothesis of the existence of LA binding sites in the Na^+ channel "inactivating gate receptor" has been sustained

by studies based on site-directed mutagenesis of the IV/S6 helix [23,24,27] or in other channel regions associated with the stability of the inactivated state [11,61]. Our data support those results and provide support for the potential existence of LA binding sites in regions of that transient complex structure, in particular of the IV/S4–S5 linker. Additionally, they agree with the Guarded Receptor Hypothesis [54] of anesthesia, which assumes that LA binding is governed by the voltage-dependent rearrangements of the Na^+ channel that ought to permit access of the anesthetic to their binding sites only upon channel depolarization. This conformational rearrangement might involve the acquisition of a helical fold by the IV/S4–S5 linker. Overall, we can envisage that LA, by binding to some of the residues involved in the interaction between the "inactivation gate receptor" and the "inactivation gate particle", will prevent the channel transition back to the closed (resting) state. This is in agreement with a similar hypothesis, based on other data, which has been suggested in the past years [14,61,62].

More than that, the unveiling of the possible existence of distinct binding sites for BZC (uncharged) and LDC (charged) and the finding that the complexes originate from a combination of hydrophobic interactions with the possibility, for BZC, to form also a stable hydrogen bond, provide the molecular basis to explain the more potent anesthetic effects exhibited by BZC in relation to LDC [52,57].

In conclusion, even considering that the approach of studying the peptide in the presence of a co-solvent (TFE/H_2O, 30%/70% v/v) has an inherently limited implication, we believe these results may ultimately guide new mutagenesis and functional studies that will help to better understand, at a molecular level, not only features of the anesthetics mechanism of action, but also the structural organization of the inactivated state jointly with the conformational changes the Na^+ channels undergo in the transition from the open to the closed states.

Acknowledgments

This work has been supported by Fundação de Amparo à Pesquisa do Estado de São Paulo (FAPESP) Grant (99/11030-9, 99/07574-3 and 01/03746-6). L.F.F and T.A.P. had fellowships from FAPESP (#00/0362-0 and #00/02026-7, respectively) and E.P. from Conselho Nacional de Desenvolvimento Científico e Tecnológico.

References

[1] E. Marban, T. Yamagishi, G.F. Tomaselli, Structure and function of voltage-gated sodium channels, J. Physiol. 508 (1998) 647–657.
[2] W.A. Catterall, Cellular and molecular biology of voltage-gated sodium channels, Physiol. Rev. 72 (1992) S15–S18.
[3] H.A. Fozzard, D.A. Hanck, Structure and function of voltage-dependent sodium channels: comparison of brain II and cardiac isoforms, Physiol. Rev. 76 (1996) 887–926.
[4] C.M. Armstrong, F. Bezanilla, Inactivation of the sodium channel II. Gating current experiments, J. Gen. Physiol. 70 (1977) 567–590.
[5] J.W. West, D.E. Patton, T. Scheuer, Y. Wang, A.L. Goldin, W.A. Catterall, A cluster of hydrophobic amino acids residues required for fast Na^+ channel inactivation, Proc. Natl. Acad. Sci. U. S. A. 89 (1992) 10910–10914.
[6] G.N. Filatov, T.P. Nguyen, S.D. Kraner, R.L. Barch, Inactivation and secondary structure in the D4/S4–5 region of the SkM1 sodium channel, J. Gen. Physiol. 111 (1998) 703–715.
[7] M.R. Smith, A.L. Goldin, Interaction between the sodium channel inactivation linker and domain III S4–S5, Biophys. J. 73 (1997) 1885–1895.
[8] H. Lerche, W. Peter, R. Fleischhauser, U. Pika-Hartlaub, T. Malina, N. Mitrovic, F. Lehmann-Horn, Role in fast inactivation of the IV/S4–S5 loop of the human muscle Na^+ channel probed by cysteine mutagenesis, J. Physiol. 505 (1997) 345–352.
[9] L. Tang, R.G. Kallen, R. Horn, Role of an S4–S5 linker in sodium channel inactivation probed by mutagenesis and a peptide blocker, J. Gen. Physiol. 108 (1996) 89–104.
[10] J.C. McPhee, D.S. Ragsdale, T. Scheuer, W.A. Catterall, A critical role for the S4–S5 intracellular loop in domain IV of the sodium channel alpha-subunit in fast inactivation, J. Biol. Chem. 273 (1998) 1121–1129.
[11] N. Yang, R. Horn, Evidence for voltage-dependent S4 movement in sodium channels, Neuron 15 (1995) 213–218.
[12] N. Yang, A.L. George, R. Horn, Molecular basis of charge movement in voltage-gated sodium channels, Neuron 16 (1996) 113–122.
[13] V. Yarov-Yarovoy, J.C. McPhee, D. Idsvoog, C. Pate, T. Scheuer, W.A. Catterall, Role of amino acid residues in transmembrane segments IS6 and IIS6 of the Na^+ channel alpha subunit in voltage-dependent gating and drug block, J. Biol. Chem. 277 (2002) 35393–35401.
[14] C. Nau, G.K. Wang, Interactions of local anesthetics with voltage-gated Na^+ channels, J. Membr. Biol. 201 (2004) 1–8.
[15] L. Tang, Glutamine substitution at Alanine (1649) in the S4–S5 cytoplasmic loop of domain 4 removes the voltage sensitivity of fast inactivation in the human heart sodium channel, J. Gen. Physiol. 111 (1998) 639–651.
[16] T. Narahashi, D.T. Frazier, M. Yamada, The site of action and active form of local anesthetics: I. Theory and pH experiments with tertiary compounds, J. Pharmacol. Exp. Ther. 171 (1970) 32–44.
[17] D.T. Frazier, T. Narahashi, M. Yamada, The site of action and active form of local anesthetics: II. Experiments with quaternary compounds, J. Pharmacol. Exp. Ther. 171 (1970) 45–51.
[18] C. Quan, W.M. Mok, G.K. Wang, Use-dependent inhibition of Na^+ currents by benzocaine homologs, Biophys. J. 70 (1996) 194–201.
[19] S.A. Godwin, J.R. Cox, S.N. Wright, Modeling of benzocaine analog interactions with the D4S6 segment of Nav4.1 voltage-gated sodium channels, Biophys. Chem. 113 (2005) 1–7.
[20] B. Hille, Local anesthetics: hydrophilic and hydrophobic pathways for the drug-receptor reaction, J. Gen. Physiol. 69 (1977) 497–515.
[21] D.E. Patton, J.W. West, W.A. Catterall, A.L. Goldin, Amino acid residues required for fast Na^+ channel inactivation: charge neutralization and deletions in the III–IV linker, Proc. Natl. Acad. Sci. U. S. A. 89 (1992) 10905–10909.
[22] G.W. Zamponi, R.J. French, Open-channel block by internally applied amines inhibits activation gate closure in batrachotoxin-activated sodium channels, Biophys. J. 67 (1994) 1040–1051.
[23] D.S. Ragsdale, J.C. McPhee, T. Scheuer, W.A. Catterall, Molecular determinants of state-dependent block of Na^+ channels by local anesthetics, Science 265 (1994) 1724–1728.
[24] G.K. Wang, C. Quan, S. Wang, A common local anesthetic receptor for benzocaine and etidocaine in voltage-gated μ1 Na^+ channels, Pflugers Arch., Eur. J. Phys. 435 (1998) 293–302.
[25] S.Y. Wang, G.K. Wang, Point mutations in segment I-S6 render voltage-gated Na^+ channels resistant to batrachotoxin, Proc. Natl. Acad. Sci. U. S. A. 95 (1998) 2653–2658.
[26] C. Nau, S.Y. Wang, G.R. Strichartz, K.G. Wang, Point mutations at N434 in DI-S6 of a Na^+ channels modulate potency and stereoselectivity of local anesthetic enantiomers, Mol. Pharmacol. 56 (1999) 404–413.
[27] D.S. Ragsdale, J.C. McPhee, T. Scheuer, W.A. Catterall, Common molecular determinants of local anesthetic, antiarrhythmic, and

anticonvulsant block of voltage-gated Na^+ channels, Proc. Natl. Acad. Sci. U. S. A. 93 (1996) 9270–9275.
[28] S.N. Wright, Localization of neurotoxin and local anesthetic receptor sites on voltage-gated sodium channels, Recent Res. Devel. Mol. Pharmacol. 1 (2002) 95–107.
[29] A. Sunami, S.C. Dudley, H.A. Fozzard, Sodium channel selectivity filter regulates antiarrhythmic drug binding, Proc. Natl. Acad. Sci. U. S. A. 94 (1997) 14126–14131.
[30] K. Miyamoto, T. Nakagawa, Y. Kuroda, Solution structures of the cytoplasmic linkers between segments S4 and S5 (S4–S5) in domains III and IV of human brain sodium channels in SDS micelles, J. Pept. Res. 58 (2001) 193–203.
[31] G. Barany, R.B. Merrifield, in: E. Gross, J. Meienhofer (Eds.), The Peptides: Analysis, Synthesis and Biology, Academic Press, New York, 1980.
[32] E. Atherton, R.C. Sheppard, Solid Phase Peptide Synthesis: A practical Approach, I.L.R. Press, Oxford, 1989.
[33] K. Wüthrich, NMR of Proteins and Nucleic Acids, John Wiley & Sons, New York, 1986.
[34] K. Nagayama, A. Kumar, K. Wüthrich, R.R. Ernst, Experimental techniques of two-dimensional correlated spectroscopy, J. Magn. Reson. 40 (1980) 321–334.
[35] C. Griesinger, G. Otting, K. Wüthrich, R.R. Ernst, Clean TOCSY for ^1H spin system identification in macromolecules, J. Am. Chem. Soc. 110 (1988) 7870–7872.
[36] G. Bodenhausen, H. Kogler, R.R. Ernst, Selection of coherence-transfer pathways in NMR pulse experiments, J. Magn. Reson. 58 (1984) 370–388.
[37] S.B. Shuker, P.J. Hajduk, R.P. Meadows, S.W. Fesik, Discovering high-affinity ligands for proteins: SAR by NMR, Science 274 (1996) 1531–1534.
[38] A.R. Waldeck, P.W. Kuchel, A.J. Lennon, B.E. Chapman, NMR diffusion measurements to characterize membrane transport and solute binding, Prog. Nucl. Magn. Reson. Spectrosc. 30 (1997) 39–68.
[39] R. Wimmer, F.L. Aachamann, K.L. Larsen, S.B. Petersen, NMR diffusion as a novel tool for measuring the association constant between cyclodextrin and guest molecules, Carbohydr. Res. 337 (2002) 841–849.
[40] P. Güntert, C. Mumenthaler, T. Herrmann, DYANA User's Manual, Institut für Molekularbiologie und Biophysik, Zürich, Switzerland, 1998.
[41] R.A. Laskowski, J.A.C. Rullmann, M.W. MacArthur, R. Kaptein, J.M. Thornton, AQUA and PROCHECK-NMR: programs for checking the quality of protein structures solved by NMR, J. Biomol. NMR 8 (1996) 477–486.
[42] E. Lindahl, B. Hess, D. van der Spoel, Gromacs 3.0: a package for molecular simulation and trajectory analysis, J. Mol. Model. 7 (2001) 306–317.
[43] H.J.C. Berendsen, J.P.M. Postma, W.F. van Gunsteren, J. Hermans, Interaction models for water in relation to protein hydration, in: B. Pullman (Ed.), Intermolecular Forces, Reidel Publishing Company, Dordrecht, 1981, pp. 331–342.
[44] M. Fioroni, K. Burger, A.E. Mark, D. Roccatano, A new 2,2,2-trifluoroethanol model for molecular dynamics simulations, J. Phys. Chem., B 104 (2000) 12347–12354.
[45] W.F. van Gunsteren, S.R. Billeter, A.A. Eising, P.H. Hünenberger, P. Krüger, A.E. Mark, W.R.P. Scott, I.G. Tironi, Biomolecular simulations: The GROMOS96 manual and user guide, vdf Hochschulverlang, ETH Zürich, Switzerland, 1996.
[46] T. Darden, D. York, L. Pedersen, Particle Mesh Ewald: an N–log(N) method for Ewald sums in large systems, J. Chem. Phys. 98 (1993) 10089–10092.
[47] T.E. Cheatham III, J.L. Miller, T. Fox, T.A. Darden, P.A. Kollman, Molecular dynamics simulations on solvated biomolecular systems: the Particle Mesh Ewald method leads to stable trajectories of DNA, RNA, and proteins, J. Am. Chem. Soc. 117 (1995) 4193–4194.
[48] B. Hess, H. Bekker, H.J.C. Berendsen, J.G.E.M. Fraaije, LINCS: a linear constraint solver for molecular simulations, J. Comput. Chem. 18 (1997) 1463–1472.
[49] S. Miyamoto, P.A. Kollman, SETTLE: an analytical version of the SHAKE and RATTLE algorithm for rigid water models, J. Comput. Chem. 13 (1992) 952–962.
[50] O. Helluin, J. Breed, H. Duclohier, Polarity-dependent conformational switching of a peptide mimicking the S4–S5 linker of the voltage-sensitive sodium channel, Biochim. Biophys. Acta 1279 (1996) 1–4.
[51] P.J. Gans, P.C. Lyer, M. Manning, R.W. Woody, N.R. Kallembach, The helix–coil transition in heterogeneous peptides with specific side-chain interactions—theory and comparison with CD spectral data, Biopolymers 31 (1991) 1605–1614.
[52] G.R. Strichartz, J.M. Ritchie, in: G.R. Strichartz (Ed.), Local Anesthetics. Handbook of experimental Pharmacology, Springer-Verlag, Berlin, 1987.
[53] M. Leuwer, G. Haeseler, H. Hecker, J. Bufler, R. Dengler, J.K. Aronson, An improved model for the binding of lidocaine and structurally related local anesthetics to fast-inactivating voltage-operated sodium channels, showing evidence of cooperativity, Br. J. Pharmacol. 141 (2004) 47–54.
[54] C.F. Starmer, Theoretical characterization of ion channel blockade: competitive binding to periodically accessible receptors, Biophys. J. 52 (1987) 405–412.
[55] B.J. Stockman, NMR spectroscopy as a tool for structure-based drug design, Prog. Nucl. Magn. Reson. Spectrosc. 33 (1998) 109–151.
[56] M. Pellechia, D.S. Sem, K. Wüthrich, NMR in drug discovery, Nat. Rev., Drug Discov. 1 (2002) 211–219.
[57] B.G. Covino, H.G. Vassalo, Local Anesthetics: Mechanisms of Action and Clinical Use, Grune and Stratton, New York, 1976.
[58] S.V.P. Malheiros, L. Gottardo, L.M.A. Pinto, D.K. Yokaichiya, L.F. Fraceto, N.C. Meirelles, E. de Paula, A new look at the hemolytic effect of local anesthetics, considering their real membrane/water partitioning at pH 7.4, Biophys. Chem. 100 (2004) 213–221.
[59] D.S. Ragsdale, M. Avoli, Brain sodium channels as molecular targets for antiepileptic drugs, Res. Brain Res. Rev. 26 (1998) 16–28.
[60] Y.M. Kuroda, K. Miyamoto, M. Matsumoto, Y. Maeda, K. Kanaori, A. Otaka, N. Fujii, T. Nakagawa, Structural study of the sodium channel inactivation gate peptide including an isoleucine–phenylalanine–methionine motif and its analogous peptide (phenylalanine/glutamine) in trifluoroethanol solutions and SDS micelles, J. Pept. Res. 56 (2000) 172–184.
[61] J.R. Balser, H.B. Nuss, D.N. Romashko, E. Marban, G.F. Tomaselli, Functional consequences of lidocaine binding to slow-inactivated sodium channels, J. Gen. Physiol. 107 (1996) 643–658.
[62] G. Haeseler, A. Piepenbrink, J. Bufler, R. Dengler, H. Hecker, J. Aronson, S. Piepenbrok, M. Leuwer, Phenol derivatives accelerate inactivation kinetics in one inactivation-deficient mutant skeletal muscle Na^+ channel, Eur. J. Pharmacol. 416 (2001) 11.